Variation in genome content and predatory phenotypes between *Bdellovibrio* sp. NC01 isolated from soil and *B. bacteriovorus* type strain HD100

Laura E. Williams[a]#, Nicole Cullen[a], Joseph A. DeGiorgis[a,b], Karla J. Martinez[a], Justina Mellone[a], Molly Oser[a]

[a]Department of Biology, Providence College, Providence, RI, USA

[b]Cellular Dynamics Program, Marine Biological Laboratory, Woods Hole, MA, USA

#Corresponding author: Laura E. Williams, lwillia7@providence.edu

Keywords: predatory bacteria, prey range, predation efficiency, plaque phenotype

Genome accession number: CP030034

Abstract

The range of naturally occurring variation in the ability of *Bdellovibrio* strains to attack and kill Gram-negative bacteria is not well understood. Defining phenotypic and associated genotypic variation among *Bdellovibrio* may further our understanding of how this genus impacts microbial communities. In addition, comparisons of the predatory phenotypes of divergent strains may inform the development of *Bdellovibrio* as biocontrol agents to combat bacterial infections. We isolated *Bdellovibrio* sp. NC01 from soil and compared its genome and predatory phenotypes to *B. bacteriovorus* type strain HD100. Based on analysis of 16S rRNA gene sequences and average amino acid identity, NC01 belongs to a different species than HD100. Genome-wide comparisons and individual gene analyses indicated that eight NC01 genome regions were likely acquired by horizontal gene transfer (HGT), further supporting an important role for HGT in *Bdellovibrio* genome evolution. Within these regions, multiple protein-coding sequences were assigned predicted functions related to transcriptional regulation and transport; however, most were annotated as hypothetical proteins. Compared to HD100, NC01 has a limited prey range and kills *E. coli* ML35 less efficiently. Whereas HD100 drastically reduces the ML35 population and then maintains low prey population density, NC01 causes a smaller reduction in ML35, after which the prey population recovers, accompanied by a decrease in NC01. In addition, NC01 forms turbid plaques on lawns of *E. coli* ML35, in contrast to clear plaques formed by HD100. Characterizing variation in interactions between *Bdellovibrio* and Gram-negative bacteria, such as observed with NC01 and HD100, is valuable for understanding the ecological significance of predatory bacteria and evaluating their effectiveness in clinical applications.

34 **Introduction**

35 Since their discovery in the early 1960s, predatory bacteria have been isolated from a
36 wide range of terrestrial and aquatic environments, including some with extreme conditions such
37 as high temperature or salinity (1). The impact of predatory bacteria in these environments is not
38 fully known, but recent studies indicate they may play an important role in shaping microbial
39 communities (2–4). In addition, their ability to attack and kill Gram-negative bacterial pathogens
40 has generated interest in developing predatory bacteria as biocontrol agents to combat drug-
41 resistant infections (5–7). Given their potential ecological significance and possible clinical
42 applications, it is important to define phenotypic and genotypic variation among predatory
43 bacteria. In particular, variation in predatory phenotypes such as prey range and predation
44 efficiency will affect how different strains of predatory bacteria impact microbial communities,
45 and this phenotypic variation may be determined by variation in genome content. To further our
46 understanding of phenotypic and genome variation in predatory bacteria, we isolated, assayed
47 and sequenced a *Bdellovibrio* strain from soil and compared its predatory phenotypes and
48 genome content to other sequenced *Bdellovibrio*.

49 Among the different genera of predatory bacteria, *Bdellovibrio* is the most well-studied.
50 Currently, this genus includes two species that differ in their predation strategy. *B. bacteriovorus*
51 invades the periplasm of Gram-negative prey cells (8), whereas *B. exovorus* attaches to the
52 outside of prey cells but does not enter the cell itself (9). Here, we focus on intraperiplasmic
53 *Bdellovibrio*. This lifecycle includes two main phases: the attack phase and the growth phase
54 (10). During the attack phase, small, highly motile *Bdellovibrio* cells seek out and attach to
55 Gram-negative prey bacteria. *Bdellovibrio* then invades the prey periplasm by using lytic
56 enzymes to open a small hole in the prey outer membrane and cell wall (11). Both attachment

57 and invasion may be mediated by Type IV pili expressed by *Bdellovibrio* (12, 13). After
58 *Bdellovibrio* moves into the prey periplasm, it uses peptidoglycan-modifying enzymes to reseal
59 and reshape the prey cell wall, resulting in formation of a rounded structure called a bdelloplast
60 (14). Within the bdelloplast, *Bdellovibrio* initiates the growth phase, during which it secretes
61 lytic enzymes into the prey cytoplasm. Using digested prey cell contents as nutrients,
62 *Bdellovibrio* grows into a single long filament within the prey periplasm, eventually dividing into
63 multiple progeny, which lyse the bdelloplast and emerge as new attack phase cells.

64 By invading and lysing Gram-negative bacteria, some strains of *Bdellovibrio* can reduce
65 prey populations by up to 8 log units over 48 hours *in vitro* (6, 15). However, not all *Bdellovibrio*
66 strains are equally effective at killing the same Gram-negative species. Researchers have
67 observed variation among *Bdellovibrio* strains in which Gram-negative bacteria are susceptible
68 to predation (16, 17) and in how quickly and to what extent a population of Gram-negative prey
69 is reduced (15, 18). These predatory phenotypes, referred to as prey range and predation
70 efficiency, are clearly important in determining the outcomes of interactions between
71 *Bdellovibrio* and Gram-negative bacteria; however, the extent of naturally occurring variation in
72 these phenotypes and the underlying mechanisms governing them are not well understood.
73 Defining how predatory phenotypes differ among *Bdellovibrio* will contribute to our
74 understanding of the impact of predatory bacteria on microbial communities in different
75 environments and inform their application in biocontrol of bacterial pathogens.

76 Here, we describe isolation of *Bdellovibrio* sp. NC01 from soil and compare its genome
77 and predatory phenotypes to other *Bdellovibrio*, focusing primarily on the *B. bacteriovorus* type
78 strain HD100. The intraperiplasmic predator HD100 was the first *Bdellovibrio* strain sequenced
79 (19), and multiple studies have dissected some of the molecular mechanisms governing predation

80 in this strain (20). To investigate variation in genome content, we compared the genome of NC01
81 to that of HD100 and *B. bacteriovorus* W (21), which is phylogenetically divergent from HD100
82 and all other fully sequenced intraperiplasmic *Bdellovibrio* (22). To define variation in predatory
83 phenotypes between NC01 and HD100, we determined prey range by testing each strain against
84 a panel of Gram-negative bacteria, and we measured predation efficiency by quantifying viable *E.*
85 *coli* ML35 during co-culture with each strain.

86 **Methods**

87 **Isolation and identification of environmental bacteria for use as prey**

88 We isolated bacteria from an urban freshwater stream in Providence, RI (lat 41.835, lon -
89 71.44299) and from soil in a residential area of Massachusetts (lat 42.0877, lon -71.2309) for use
90 as prey. We also obtained *E. coli* ML35 from Mark Martin (University of Puget Sound, Puget
91 Sound, WA) and *Escherichia* 0057 from Brett Pellock (Providence College, Providence, RI).

92 To identify these isolates, we sequenced the 16S rRNA gene following a previously
93 described procedure (23). Briefly, we used primers 63F (24) and 1378R (25), which amplify the
94 16S rRNA gene from many members of Domain Bacteria. Sanger sequencing of purified PCR
95 products was performed by GeneWiz (South Plainfield, NJ) using the same primers. We trimmed
96 and assembled reads using Phred/Phrap/Consed (26–28), then classified the assembled 16S
97 rRNA gene sequences using BLAST (29), the SILVA Incremental Aligner (30) and the
98 Ribosomal Database Project classifier (31). Supplementary Table 1 shows the full classification
99 results. The RDP classifier and the SILVA Incremental Aligner classify sequences to the genus
100 level, but not the species level; therefore, species names are not provided for these isolates.

101 **Isolation and identification of *Bdellovibrio* sp. NC01 from bioswale soil**

102 In September 2015, we collected 50 g of soil from a bioswale on the Providence College
103 campus (lat 41.84277, lon -71.43944). To isolate predatory bacteria from the soil sample, we
104 adapted standard methods (32, 33). We combined the soil sample with 500 ml of sterile HM
105 buffer (25 mM HEPES adjusted to pH 7.4 and supplemented with 3 mM calcium chloride
106 dihydrate and 2 mM magnesium chloride hexahydrate). We then filtered this mixture through
107 sterile cheesecloth into a sterile container to remove large particulate matter. We vortexed the
108 filtrate to release bacterial cells from the small particles of soil that passed through the
109 cheesecloth. To pellet the soil particles, we centrifuged the filtrate at 1753 rpm for 10 minutes,
110 after which we retained the supernatant containing suspended bacterial cells.
111 To enrich for predatory bacteria in the soil sample supernatant, we used *Pseudomonas* sp.
112 NC02 as prey, because it was also isolated from a soil environment, and its genome has been
113 sequenced (34). We cultured *Pseudomonas* sp. NC02 overnight in 120 ml tryptic soy broth
114 (TSB) at 28°C and 200 rpm, then centrifuged the culture at 6000 rpm for 10 minutes, washed the
115 resulting pellet with 100 ml sterile HM buffer, centrifuged again and resuspended the resulting
116 pellet in 2.5 ml HM buffer. We combined 1 ml of *Pseudomonas* sp. NC02 resuspension with 20
117 ml of soil sample supernatant and incubated this enrichment at 28°C and 200 rpm.
118 Once we observed small, fast-moving cells under 1000x phase-contrast microscopy, we
119 filtered the enrichment using a 0.45 μm filter and performed 10-fold serial dilutions of the filtrate
120 in sterile HM buffer. Dilutions were then plated using a double agar overlay method. For each
121 dilution of the filtrate to be plated, we combined 100 μl of the dilution, 250 μl of *Pseudomonas*
122 sp. NC02 at 10^8 cfu/ml and 4.5 ml of molten HM top agar (0.6% agar). After vortexing, we
123 poured this mixture onto HM agar plates (1.5% agar). We allowed the top agar to solidify at
124 room temperature, then incubated plates at 28°C until we observed plaques in the lawn of

125 *Pseudomonas* sp. NC02. To begin the process of obtaining a pure isolate, we used a sterile
126 Pasteur pipette to extract single, well-defined plaques from the top agar. We combined each
127 plaque with 500 μl of sterile HM buffer, incubated the plaque suspension at room temperature
128 for at least 5 minutes, then vortexed it vigorously.

129 To culture predatory bacteria from the plaque suspensions, we made lysates combining
130 300 μl of each plaque suspension, 1.5 ml of an overnight culture of *Serratia* 0043 and 20 ml
131 sterile HM buffer. *Serratia* 0043 was also isolated from a soil environment, and switching to this
132 prey species during the isolation procedure selected for predatory isolates that were capable of
133 attacking both *Pseudomonas* and *Serratia*, which belong to different orders. We incubated
134 lysates at 28°C and 200 rpm. After 48 h, one lysate showed small, fast-moving cells, and we
135 used this lysate to begin two additional rounds of serial dilution, plating and plaque picking to
136 ensure a pure isolate. We used *Serratia* 0043 as prey during both of these rounds. After the final
137 round, we filtered the plaque suspension using a 0.45 μm filter, then combined 500 μl of filtrate
138 with 500 μl of sterile 50% glycerol and stored the stock at -80°C.

139 To identify NC01, we extracted the 16S rRNA gene sequence from the NC01 genome
140 based on the annotation generated by PGAP (see below for genome sequencing and annotation
141 methods). Using SINA 1.2.11 (30), we aligned this sequence against 16S rRNA gene sequences
142 extracted from nine genomes of obligate predatory bacteria belonging to *Bacteriovorax*,
143 *Bdellovibrio* and *Halobacteriovorax* (*Bacteriovorax stolpii* DSM12778 CP025704, *Bdellovibrio*
144 *bacteriovorus* 109J CP007656, *Bdellovibrio bacteriovorus* HD100 NC_005363, *Bdellovibrio*
145 *bacteriovorus* SSB218315 CP020946, *Bdellovibrio bacteriovorus* Tiberius NC_019567,
146 *Bdellovibrio bacteriovorus* W NZ_CP002190, *Bdellovibrio exovorus* JSS NC_020813,
147 *Halobacteriovorax marinus* BE01 CP017414, *Halobacteriovorax marinus* SJ NC_016620). We

148 then inferred a phylogeny from the alignment with the online server RAxML Blackbox (35),
149 using 100 bootstrap replicates to estimate the confidence of the topology.
150 To further investigate the relationships among NC01 and other *Bdellovibrio*, we used an
151 average amino acid identity (AAI) calculator (http://enve-omics.ce.gatech.edu/) (36) to analyze
152 the similarity among protein-coding sequences from NC01, 109J, HD100 and W, as annotated by
153 RAST (see below for genome sequencing and annotation methods).

154 **Negative stain electron microscopy of *Bdellovibrio* sp. NC01**

155 To obtain samples of *Bdellovibrio* sp. NC01 for negative stain electron microscopy, we
156 added a small amount of the -80°C freezer stock to 20 ml of HM buffer mixed with 1.5 ml of an
157 overnight culture of *E. coli* ML35 grown in TSB. After 48 h of incubation at 28°C and 200 rpm,
158 we stained samples with uranyl acetate following a previously described procedure (23) and
159 imaged the resulting specimens using a JEOL CX 2000 transmission electron microscope.

160 **Genome sequencing, annotation and analysis of *Bdellovibrio* sp. NC01**

161 To obtain genomic DNA, we combined a small amount of the -80°C stock, 1.5 ml of an
162 overnight culture of *E. coli* ML35 and 25 ml of sterile HM buffer. We chose ML35 as prey
163 because it is a standard prey strain used in cultivation of *Bdellovibrio*, and the genome sequence
164 is available for screening reads if needed (37). After 72 hours of incubation at 28°C and 200 rpm,
165 we centrifuged the lysate at 9100 rpm for 10 minutes to pellet bacterial cells. Because PacBio
166 sequencing technology requires at least 10 μg of genomic DNA, we did not filter the lysate to
167 prevent loss of predatory bacteria cells. We then used the Wizard Genomic DNA purification kit
168 to extract genomic DNA, following the manufacturer's instructions beginning with resuspension
169 of the pellet in 600 μl of the kit's nuclei lysis solution. For the final rehydration step, we

170 rehydrated the DNA pellet overnight at 4°C. Quantification by Qubit estimated a final
171 concentration of 340 ng/μl genomic DNA.
172 For long-read sequencing, library construction and sequencing were performed at the
173 Institute for Genome Sciences at the University of Maryland Baltimore on a Pacific Biosciences
174 RSII instrument using P6-C4 chemistry. Quality control analysis of the reads showed that <10%
175 of reads aligned by BLAST to *E. coli* or *Shigella*, indicating that representation of the prey
176 genome in the read dataset is low. To analyze and assemble the reads, we launched an instance
177 of SMRT Portal 2.3.0 using Amazon EC2. A single SMRT cell yielded 79,088 postfilter
178 polymerase reads (N_{50} 17,028) and 94,031 subreads (N_{50} 13,572). Within SMRT Portal, we
179 assembled the reads with HGAP3 (38), using 4.5 Mbp for the genome size. This generated 186
180 contigs. The largest contig was 4,001,137 bp and aligned to *Bdellovibrio* in the database using
181 BLASTN. The other 185 contigs were each <48,000 bp in length, and all of them aligned to *E.*
182 *coli* by BLASTN, which is expected due to the inclusion of prey genomic DNA in the
183 sequencing library.
184 To close the genome, we used BLASTN to identify overlap in the ends of the contig and
185 trimmed the sequence to generate a closed contig of 3,975,771. We also adjusted the start site so
186 that the first nucleotide of the closed genome sequence corresponds to the first nucleotide in the
187 start codon of *dnaA*. To polish this sequence, we used 250 bp paired-end Illumina MiSeq data
188 generated at the Rhode Island Genomics and Sequencing Center. We filtered and trimmed the
189 raw read dataset to retain only those read pairs for which the quality score of every base was ≥13
190 and the read length was ≥65. This yielded 1,256,135 read pairs. Using bwa-mem (39), samtools
191 (40) and Pilon (41), we aligned these reads to the closed genome sequence and corrected 1 SNP,
192 84 small insertions totaling 85 bases and 4 small single-base deletions. We manually examined

193 changes flagged by Pilon using the alignment viewer Tablet (42), generating a final, polished
194 *Bdellovibrio* sp. NC01 genome sequence of 3,975,853 bp. This sequence has been deposited in
195 GenBank as CP030034.

196 In addition to annotation with NCBI's Prokaryotic Genome Annotation Pipeline (PGAP)
197 version 4.5, we also annotated the sequence using ClassicRAST (43, 44), Infernal (45), and
198 tRNAScan-SE (46, 47). For genome-wide pairwise comparisons, we used the BLAST Ring
199 Image Generator (BRIG) (48).

200 **Phenotype assays to test prey range and predation efficiency**

201 We obtained *Bdellovibrio bacteriovorus* HD100 from Mark Martin (University of Puget
202 Sound, Puget Sound, WA) for predatory phenotype comparisons. To conduct phenotype assays,
203 we adapted standard methods (32, 33, 49). To culture *Bdellovibrio* NC01 and HD100, we added
204 a small amount of -80°C stocks to 20 ml HM buffer combined with 1.5 ml of an overnight
205 culture of *E. coli* ML35. After 72 hours of incubation at 28°C and 200 rpm, we filtered the lysate
206 using a 0.45 μm filter to separate predatory cells from prey cells and cell debris. For each
207 phenotype assay described below, we followed this protocol to obtain attack phase *Bdellovibrio*
208 cells.

209 To test prey range and plaque appearance, we plated 10-fold serial dilutions of filtered
210 lysate using a double agar overlay method as described above for the isolation procedure. Each
211 tested prey strain was grown in 120 ml TSB overnight at 28°C and 200 rpm, with the exception
212 of *Escherichia* strains, which were grown at 37°C. After centrifugation and washing, we
213 resuspended prey cell pellets in 5 ml of sterile HM buffer. Based on cfu/ml counts, this yielded
214 concentrations of at least 10^8 cfu/ml, which ensured a dense prey lawn for visualizing plaques.
215 For some prey strains, we added 500 μl of prey resuspension to top agar to improve our ability to

216 detect and observe plaques in the prey lawn. We incubated plates at 28°C for 8 days before
217 scoring plaque formation and performed three replicates for each prey strain. In observations of
218 plaque appearance, we photographed plates at multiple time points over the course of 8 days.
219 To test predation efficiency, we adapted a protocol described in (18). We centrifuged the
220 filtered lysate at 8500 rpm for 10 minutes. The resulting pellet of predatory bacteria was
221 resuspended in sterile HM buffer to yield ~10^8 cells/ml based on direct cell counts using a
222 Petroff-Hausser counting chamber and 1000x phase-contrast microscopy. To ensure that direct
223 cell counts provided accurate estimates of active predatory bacteria concentrations, we validated
224 the method by comparing cells/ml estimated using the Petroff-Hausser counting chamber with
225 plaque-forming units/ml estimated using serial dilution and double agar overlay to count plaques
226 in a prey lawn. Results from two replicates showed that direct cell counts were slightly lower
227 than pfu/ml counts, but within the same order of magnitude (direct cell counts: 3.94 x 10^8
228 cells/ml and 2.58 x 10^8 cells/ml, plaque counts: 9.2 x 10^8 pfu/ml and 4.7 x 10^8 cells/ml).
229 To initiate the predation efficiency assay, we combined 500 µl of *Bdellovibrio* cell
230 resuspension (at ~10^8 cells/ml) with 12.5 ml of an overnight culture of *E. coli* ML35 diluted to
231 OD_{600} 0.15 (range: 0.135 – 0.165). This yielded ~10^8 cfu/ml, therefore the predation efficiency
232 assay results reported here are based on a predator:prey ratio of approximately 1:1. As a control,
233 we used 500 µl of sterile HM buffer in place of *Bdellovibrio* cell resuspension. Using cfu/ml
234 counts, we quantified viable *E. coli* ML35 at the beginning of the assay (time zero) and then after
235 6, 24, 48 and 72 hours of incubation at 28°C and 200 rpm.

236 **Results**

237 **Bioswale soil harbors predatory bacteria belonging to *Bdellovibrio***

238 Using Gram-negative soil bacteria isolated from a residential area as prey, we performed
239 an enrichment followed by three rounds of plaque picking to obtain a pure isolate of predatory
240 bacteria from a sample of soil collected at a bioswale on the Providence College campus. The
241 bioswale is a manmade landscape feature designed to collect and filter stormwater runoff from
242 nearby buildings. We designated the bioswale soil isolate as NC01. Using 1000x phase-contrast
243 microscopy of lysates combining NC01 and Gram-negative prey, we observed small, fast-
244 moving attack phase NC01 cells that attached to prey cells (Figure 1a). We also observed
245 rounded structures characteristic of bdelloplasts, suggesting that NC01 uses a cell invasion
246 strategy similar to *Bdellovibrio bacteriovorus*. Negative stain electron microscopy showed that
247 NC01 attack phase cells have a comma-shaped morphology with a single polar flagellum (Figure
248 1b).

249 To identify NC01, we constructed a phylogeny of 16S rRNA gene sequences from this
250 isolate and nine *Bacteriovorax*, *Bdellovibrio* and *Halobacteriovorax* strains with complete
251 genomes available in GenBank (Figure 2). In this phylogeny, NC01 clearly clusters with other
252 *Bdellovibrio*. Pairwise alignment of 16S rRNA gene sequences from NC01 and *Bdellovibrio*
253 *bacteriovorus* HD100, which is the type strain of the species, showed 97% similarity across
254 1,516 nucleotides. This value is above the 95% similarity cutoff typically used to define bacterial
255 genera (50), which supports identifying NC01 as *Bdellovibrio*. However, it is below the 98.7%
256 similarity cutoff typically used to define species (51), which suggests that NC01 belongs to a
257 different species than *bacteriovorus*.

258 To explore this further, we compared the average amino acid identity (AAI) of
259 *Bdellovibrio* strains NC01, W, HD100 and 109J (Table 1). HD100 and 109J, which are both
260 identified as *B. bacteriovorus*, cluster in a well-supported clade in the 16S rRNA phylogeny, and

261 their protein sequences are highly similar (average AAI 99.2%). However, NC01 protein
262 sequences are <70% similar on average to HD100 and 109J protein sequences, supporting the
263 conclusion that NC01 belongs to a different species than these two strains. NC01 protein
264 sequences are even less similar on average to those of strain W, suggesting that NC01 does not
265 belong to the same species as this strain. Based on these analyses, we chose not to designate a
266 species for NC01, and we refer to this isolate as *Bdellovibrio* sp. NC01.

267 **Comparative genomics identifies eight regions of unique gene content possibly acquired by**
268 ***Bdellovibrio* sp. NC01 via horizontal gene transfer**

269 Based on the 16S rRNA gene phylogeny and average AAI comparisons, we chose *B.*
270 *bacteriovorus* HD100 and *B. bacteriovorus* W to represent phylogenetic diversity and genome
271 variation among intraperiplasmic *Bdellovibrio* for comparative genomics. The genome of
272 *Bdellovibrio* sp. NC01 is larger than that of both HD100 and W (Table 2). The GC content of the
273 NC01 genome is lower than that of HD100, but slightly higher than that of W. Using the BLAST
274 Ring Image Generator (BRIG), we conducted pairwise comparisons of NC01 to HD100 and W
275 based on nucleotide sequence alignments with BLASTN. This analysis identified eight NC01
276 genome regions of at least 15,000 nucleotides in which no alignments of >200 nucleotides and e-
277 value <0.1 to HD100 or W were reported. These eight regions, which may represent unique
278 NC01 gene content, are marked on Figure 3. The plot of GC content shows that four of the eight
279 regions (regions 1, 4, 5, and 7) encompass substantial decreases in GC content compared to the
280 typical variation along the genome. Such deviation in GC content may be an indicator of
281 horizontal gene transfer (HGT) (52).

282 To assess whether the genes encoded in these eight NC01 genome regions are present but
283 divergent in HD100 and W, we used TBLASTN to compare NC01 amino acid sequences

284 annotated in each region by RAST to the HD100 and W genomes translated into all six reading
285 frames. RAST annotated 11 to 50 protein-coding sequences within each of the eight NC01
286 genome regions. By searching for these sequences along the entire HD100 and W genomes, this
287 analysis detects similar protein-coding sequences even if the genes have undergone
288 rearrangement. For the majority of the protein-coding sequences in each of the eight NC01
289 regions, TBLASTN did not produce any alignments to HD100 or W with >70% query coverage.
290 For those protein-coding sequences that did align to HD100 and/or W with >70% query coverage,
291 identity was low (<40%) for most of the sequences. Less than five protein-coding sequences in
292 each region aligned to HD100 or W at >70% coverage and >40% identity. This suggests that the
293 protein-coding sequences in the eight NC01 genome regions are missing from HD100 and W,
294 instead of divergent.

295 In addition to comparisons against HD100 and W, we also used BLASTP to align amino
296 acid sequences annotated in each region by RAST against the non-redundant GenBank database.
297 For each sequence, we examined the top 250 alignments for any sequences identified as
298 *Bdellovibrio*. This analysis expands the search space beyond complete *Bdellovibrio* genomes to
299 any deposited sequences that were denoted by the submitters as *Bdellovibrio*. In two of the
300 regions (regions 1 and 4), only one-third of amino acid sequences aligned to *Bdellovibrio*
301 sequences. In every other region except region 8, 52-64% of the amino acid sequences aligned to
302 *Bdellovibrio* sequences. In region 8, three-fourths of the amino acid sequences aligned to
303 *Bdellovibrio* sequences. These results suggest that most of the protein-coding sequences in
304 regions 1 and 4 may be unique to *Bdellovibrio* sp. NC01, because they do not align to other
305 *Bdellovibrio* sequences in the database. In the other regions, the larger proportion of shared gene

306 content between NC01 and *Bdellovibrio* in the database may be the result of HGT events that
307 occurred before the divergence of NC01 and these strains.

308 The hypothesis that the eight NC01 genome regions were acquired by horizontal gene
309 transfer is also supported by predicted functions of the protein-coding sequences encoded within
310 the regions. RAST annotation identified functions related to mobile elements in five of the eight
311 regions. These include phage tail fibers (regions 1, 5 and 6), site-specific recombinases or
312 integrases (regions 1, 4, and 7), a phage-related DNA primase (region 4), and a plasmid
313 conjugative transfer protein (region 7). In addition, Prophinder analysis of the complete NC01
314 genome identified a portion of region 5 (1,632,099 – 1,632,833) as a possible prophage. Three
315 regions (regions 2, 3 and 8) did not encode any obvious mobile element functions.

316 Apart from mobile element-related genes, most of the protein-coding sequences in the
317 eight NC01 genome regions are annotated as hypothetical proteins, therefore it is unclear what
318 functional capacities may have been gained by *Bdellovibrio* sp. NC01 via HGT and whether
319 those functions impact predation. Some of the genes were annotated with predicted functions,
320 which enabled us to assess gene content in the eight regions in terms of broad functional
321 categories. Four of the eight regions (regions 1, 3, 6 and 8) encode predicted functions related to
322 transcriptional regulation, and five regions (regions 1, 3, 5, 6, and 7) encode predicted functions
323 related to transport. Regarding enzymatic activity, region 6 encodes a predicted cell wall
324 endopeptidase, which is interesting given *Bdellovibrio*'s interactions with the Gram-negative
325 prey cell wall during its life cycle.

326 ***Bdellovibrio* sp. NC01 has a limited prey range compared to HD100 and is less efficient at**
327 **killing *E. coli* ML35**

328 To assess variation in predatory phenotypes between *Bdellovibrio* sp. NC01 and *B.*
329 *bacteriovorus* HD100, we assayed prey range and predation efficiency. To determine prey range,
330 we tested NC01 and HD100 against a panel of eight Gram-negative bacteria isolated from
331 different environments, including a freshwater stream and soil from a residential area (Table 3).
332 Plaque formation on a bacterial lawn indicates that the predatory isolate is able to attack and lyse
333 that particular Gram-negative prey strain. NC01 formed plaques on lawns of five of the eight
334 prey strains tested, whereas HD100 formed plaques on lawns of all eight prey strains. NC01 was
335 not able to attack and lyse two prey strains belonging to *Acinetobacter* and *Raoultella* that were
336 isolated from a freshwater stream. In addition, although NC01 formed plaques on *E. coli* ML35,
337 it did not attack and lyse *E. coli* 0057.
338 To measure predation efficiency, we quantified viable *E. coli* ML35 by calculating cfu/ml
339 at different time points over 72 hours of co-culture with NC01 or HD100 (Figure 4). In the
340 absence of predatory bacteria, we did not observe any reduction in viable *E. coli* ML35,
341 demonstrating that co-culture conditions do not adversely affect the ML35 population. After 6
342 hours of co-culture, NC01 did not appreciably reduce viable *E. coli* ML35 compared to the
343 control, whereas HD100 reduced viable ML35 by approximately 1 log unit. After 24 hours of co-
344 culture, there was a substantial difference in the impact of NC01 and HD100 on the *E. coli*
345 population. NC01 reduced viable ML35 by approximately 3 log units compared to the control,
346 whereas HD100 reduced viable ML35 by 6 log units. Over the next 48 hours, HD100 continued
347 to restrict the viable ML35 population, but the population recovered in co-cultures with NC01,
348 increasing by 2 log units. ML35 population recovery in the presence of NC01 was consistently
349 observed in all assay replicates, and cfu/ml plates showed no evidence of contaminant bacteria.

350 For two of the assay replicates, we quantified NC01 and HD100 after 72 hours of co-
351 culture to determine if recovery of the ML35 population is associated with changes in predatory
352 bacteria population density. Based on direct cell counts used to establish co-cultures, both NC01
353 and HD100 populations were ~10^8 cells/ml at the beginning of the assay (NC01: 3.8 x 10^8
354 cells/ml and 7.8 x 10^8 cells/ml, HD100: 4.1 x 10^8 cells/ml and 9.8 x 10^8 cells/ml). After 72 hours
355 of co-culture with *E. coli* ML35, plaque counts showed a small decrease in the HD100
356 population (1.5 x 10^8 pfu/ml and 4.5 x 10^8 pfu/ml), whereas the NC01 population decreased
357 substantially (2.3 x 10^5 pfu/ml and 7.5 x 10^6 pfu/ml). When compared in validation tests, direct
358 cell counts and plaque counts yielded comparable results, therefore the observed decrease in
359 NC01 population is not due to a difference in methods for determining predator population
360 density. These data demonstrate that for both NC01 and HD100, active predatory bacteria are
361 present after 72 hours of co-culture with *E. coli* ML35, but, in contrast to HD100, the NC01
362 population density decreases by at least two orders of magnitude over the course of the predation
363 efficiency assay.

364 **Plaques formed by *Bdellovibrio* sp. NC01 on *E. coli* ML35 prey lawns are not as clear as**
365 **those formed by HD100**

366 In addition to quantitative differences in the ability of *Bdellovibrio* sp. NC01 and *B.*
367 *bacteriovorus* HD100 to kill *E. coli* ML35, we also observed qualitative differences in the
368 appearance of plaques formed by each strain on lawns of ML35 (Figure 5). In contrast to HD100,
369 which forms completely clear, regular plaques, NC01 forms plaques of a similar size, but with
370 incomplete clearance of the prey lawn within the plaques. Some NC01 plaques remain
371 completely turbid over eight days of incubation, whereas others retain a turbid center but begin
372 to clear on the edges of the plaque.

373 **Discussion**

374 We isolated *Bdellovibrio* from soil collected at a manmade landscape feature designed for
375 stormwater management on a college campus. By comparing 16S rRNA gene sequences and
376 analyzing average amino acid identity (AAI) among multiple sequenced *Bdellovibrio*, we
377 determined that the *Bdellovibrio* isolate was sufficiently divergent from *B. bacteriovorus* type
378 strain HD100 and other *B. bacteriovorus* strains that it should be identified as a different species.
379 The only other species currently described within *Bdellovibrio* is *exovorus*; however, this species
380 uses an epibiotic predation strategy that differs from the cell invasion strategy observed by
381 microscopy for the soil *Bdellovibrio* isolate described here. Pending further characterization, we
382 designated the isolate as *Bdellovibrio* sp. NC01.

383 Because *Bdellovibrio* sp. NC01 is phylogenetically divergent from HD100 and other
384 intraperiplasmic *Bdellovibrio* with sequenced genomes, this isolate provides a valuable
385 opportunity to assess variation in genome content and predatory phenotypes among *Bdellovibrio*.
386 Genome-wide comparisons of NC01 to HD100 and W using BLASTN identified eight regions of
387 unique gene content along the NC01 genome, and TBLASTN confirmed that the protein-coding
388 sequences within these regions are missing from the genomes of HD100 and W. Multiple lines of
389 evidence support the hypothesis that these eight regions were acquired by *Bdellovibrio* sp. NC01
390 via horizontal gene transfer. Four of the regions have substantially lower GC content than the
391 genome average, which may indicate horizontal acquisition from a bacterial genome with a
392 lower average GC content than that of NC01 (52). Five of the regions encode genes with
393 predicted functions related to mobile elements such as phage and plasmids, and one of these
394 regions was identified as a possible prophage by phage finding sequence analysis software.

395 Alignment by BLASTP of amino acid sequences encoded within two of the eight regions
396 against the GenBank database suggested that these two regions may have been acquired recently
397 by *Bdellovibrio* sp. NC01, because most of the sequences did not align to *Bdellovibrio* sequences
398 (complete or partial) in the database. This indicates that, given the current representation of
399 *Bdellovibrio* in the database, gene content in these two regions is mostly unique to NC01. For the
400 other six regions, the majority of amino acid sequences encoded in these regions aligned to
401 *Bdellovibrio* sequences in the database. This suggests that these *Bdellovibrio* strains may be
402 closely related to NC01, and the HGT events corresponding to acquisition of these six regions
403 occurred in the ancestral lineage before NC01 diverged from these strains. Addition of more
404 complete *Bdellovibrio* genomes to the database will improve our ability to reconstruct
405 evolutionary events such as horizontal gene transfer.
406 The analysis of *Bdellovibrio* sp. NC01 gene content reported here further illustrates the
407 role of horizontal gene transfer as an important force in predatory bacteria genome evolution.
408 Comparative genomics has yielded evidence of both ancient and recent HGT in *Bdellovibrio* and
409 in the saltwater-adapted predatory genus *Halobacteriovorax* (23, 53–55). However, lack of
410 functional annotation of many *Bdellovibrio* protein-coding sequences prevents a thorough
411 assessment of how HGT events impact predatory phenotypes. Within the eight NC01 genome
412 regions likely acquired via HGT, many of the protein-coding sequences are annotated as
413 hypothetical proteins, which provides no insight into their function and their potential roles in the
414 predatory life cycle. To fully understand how *Bdellovibrio* genome variation relates to variation
415 in predatory phenotypes, it is essential to assign functions to protein-coding genes.
416 In addition to genome comparisons, we also compared predatory phenotypes between
417 *Bdellovibrio* sp. NC01 and *B. bacteriovorus* type strain HD100. Based on plaque formation on

418 lawns of eight different Gram-negative bacteria, NC01 has a more restricted prey range than
419 HD100. In particular, HD100 was able to attack and kill both tested strains of *E. coli*, whereas
420 NC01 was only able to attack and kill *E. coli* ML35. Other researchers have also observed that a
421 particular *Bdellovibrio* strain may vary in its ability to kill different members of the same species
422 (16, 56); however, the mechanisms governing these outcomes are not known. By demonstrating
423 that strain-level variation within a Gram-negative species determines susceptibility to predation,
424 these data have potentially important implications for developing predatory bacteria as
425 biocontrol agents in the treatment of bacterial infections. If a *Bdellovibrio* isolate attacks and
426 kills one representative of a Gram-negative species, it does not guarantee that the isolate will
427 attack and kill other strains within the species. Further work to define the molecular mechanisms
428 underlying variation in prey range may enable prediction of whether a Gram-negative strain will
429 be susceptible to predation by a particular *Bdellovibrio* strain.

430 Although both NC01 and HD100 can attack and kill *E. coli* ML35, predation by HD100
431 causes a greater reduction in the ML35 population after 24 hours *in vitro* compared to predation
432 by NC01. HD100 then maintains a low ML35 population density, although it does not
433 completely eliminate viable ML35. By contrast, in co-cultures of NC01 and ML35, the ML35
434 population recovers after 24 hours, whereas the NC01 population decreases. This is likely not the
435 result of general predator-prey dynamics, such as an increase in search time due to reduced
436 ML35 numbers, because we did not observe ML35 population recovery in co-cultures with
437 HD100. Other researchers have observed similar prey population recovery (57, 58), and
438 Shemesh and Jurkevitch demonstrated that recovery of *Erwinia carotovora* in co-cultures with
439 *Bdellovibrio* isolated from soil was due to development of phenotypic resistance to predation. It
440 is possible that *E. coli* ML35 uses a similar mechanism to develop resistance to predation by

441 *Bdellovibrio* sp. NC01, thereby causing the NC01 population to decrease as a result of starvation
442 due to lack of susceptible prey. This mechanism is either not expressed or not successful in co-
443 cultures with *B. bacteriovorus* HD100. Further work will test this hypothesis and define the
444 molecular mechanisms governing ML35 population recovery.

445 Differences in predation efficiency between NC01 and HD100 on *E. coli* ML35 may also
446 be related to variation in plaque phenotype. Plaques formed by NC01 on lawns of ML35 are
447 turbid, whereas plaques formed by HD100 are completely clear. Turbid plaques have been
448 reported as a characteristic of prey-independent mutants of *Bdellovibrio*; however, these plaques
449 are typically smaller than those formed by the wild-type strain and sometimes have a small
450 colony of host-independent *Bdellovibrio* at their center (59, 60). Neither of these features were
451 observed when comparing NC01 and HD100 plaques, suggesting that the NC01 plaque
452 phenotype is not the result of prey-independent growth. Turbid plaques formed by NC01 may
453 arise from incomplete lysis of *E. coli* ML35 cells. If prey cells are successfully invaded but not
454 lysed, *Bdellovibrio* progeny will be trapped, which would explain the incomplete clearance of
455 the prey lawn and the decrease in the NC01 population observed during predation efficiency
456 assays. Further work will test this hypothesis.

457 Overall, comparisons between *Bdellovibrio* sp. NC01 and *B. bacteriovorus* HD100
458 identified variation in predation phenotypes that may have important implications for the
459 ecological impact of each of these strains and their effectiveness in clinical applications. The
460 molecular mechanisms governing phenotypes such as prey range and predation efficiency are not
461 known. Comparative genomics can generate hypotheses linking gene content differences to
462 observed phenotype differences, but the lack of functional annotation for many protein-coding
463 genes complicates this effort. It is also likely that the outcomes of interactions between predatory

464 bacteria and prey, such as whether or not two different *Bdellovibrio* can kill the same Gram-
465 negative strain, are dependent upon mechanisms specific to the *Bdellovibrio* strain and
466 mechanisms specific to the prey strain. Defining these mechanisms is key for understanding
467 variation in predatory phenotypes among divergent *Bdellovibrio*.

468 **Author statements**

469 **Conflicts of interest**

470 The authors declare that there are no conflicts of interest.

471 **Funding information**

472 This research was supported by an Institutional Development Award (IDeA) from the
473 National Institute of General Medical Sciences of the National Institutes of Health under grant no.
474 P20GM103430 and by funding to LEW from Providence College. This material is based upon
475 work conducted at a Rhode Island NSF EPSCoR research facility, the Genomics and Sequencing
476 Center, supported in part by the National Science Foundation EPSCoR Cooperative Agreement
477 #EPS-1004057. This material is based upon work supported in part by the National Science
478 Foundation under EPSCoR Cooperative Agreement #OIA-1655221. The funders had no role in
479 study design, data collection and interpretation, or the decision to submit the work for
480 publication.

481 **Acknowledgements**

482 We thank Lisa Sadzewicz and Luke Tallon at the Institute for Genome Sciences at the
483 University of Maryland Baltimore for PacBio sequencing services. We thank Janet Atoyan at the
484 Rhode Island Genomics and Sequencing Center for Illumina MiSeq sequencing services. We
485 thank Sean O'Donnell for isolating freshwater prey bacteria and Mark Martin and Brett Pellock
486 for donating bacterial strains.

487 **References**

488 1. Jurkevitch E, Davidov Y. 2007. Phylogenetic diversity and evolution of predatory
489 prokaryotes, p. 11–56. *In* Jurkevitch, E (ed.), Predatory Prokaryotes: Biology, Ecology and
490 Evolution. Springer Berlin Heidelberg, Berlin, Heidelberg.

491 2. Chen H, Laws EA, Martin JL, Berhane T-K, Gulig PA, Williams HN. 2018. Relative
492 contributions of *Halobacteriovorax* and bacteriophage to bacterial cell death under various
493 environmental conditions. MBio 9.

494 3. Welsh RM, Zaneveld JR, Rosales SM, Payet JP, Burkepile DE, Thurber RV. 2016.
495 Bacterial predation in a marine host-associated microbiome. ISME J 10:1540–1544.

496 4. Feng S, Tan CH, Constancias F, Kohli GS, Cohen Y, Rice SA. 2017. Predation by
497 *Bdellovibrio bacteriovorus* significantly reduces viability and alters the microbial
498 community composition of activated sludge flocs and granules. FEMS Microbiol Ecol 93.

499 5. Dwidar M, Monnappa AK, Mitchell RJ. 2012. The dual probiotic and antibiotic nature of
500 *Bdellovibrio bacteriovorus*. BMB Rep 45:71–78.

501 6. Kadouri DE, To K, Shanks RMQ, Doi Y. 2013. Predatory bacteria: a potential ally against
502 multidrug-resistant Gram-negative pathogens. PLoS ONE 8:e63397.

503 7. Tyson J, Sockett RE. 2017. Nature knows best: employing whole microbial strategies to
504 tackle antibiotic resistant pathogens. Environmental Microbiology Reports 9:47–49.

505 8. Martin MO. 2002. Predatory prokaryotes: an emerging research opportunity. J Mol
506 Microbiol Biotechnol 4:467–477.

507 9. Koval SF, Hynes SH, Flannagan RS, Pasternak Z, Davidov Y, Jurkevitch E. 2013.
508 *Bdellovibrio exovorus* sp. nov., a novel predator of *Caulobacter crescentus*. Int J Syst Evol
509 Microbiol 63:146–151.

510 10. Sockett RE. 2009. Predatory lifestyle of *Bdellovibrio bacteriovorus*. Annu Rev Microbiol
511 63:523–539.

512 11. Kuru E, Lambert C, Rittichier J, Till R, Ducret A, Derouaux A, Gray J, Biboy J, Vollmer W,
513 VanNieuwenhze M, Brun YV, Sockett RE. 2017. Fluorescent D-amino-acids reveal bi-
514 cellular cell wall modifications important for *Bdellovibrio bacteriovorus* predation. Nat
515 Microbiol 2:1648–1657.

516 12. Mahmoud KK, Koval SF. 2010. Characterization of type IV pili in the life cycle of the
517 predator bacterium *Bdellovibrio*. Microbiology (Reading, Engl) 156:1040–1051.

518 13. Avidan O, Petrenko M, Becker R, Beck S, Linscheid M, Pietrokovski S, Jurkevitch E. 2017.
519 Identification and characterization of differentially-regulated Type IVb pilin genes
520 necessary for predation in obligate bacterial predators. Sci Rep 7:1013.

521 14. Lerner TR, Lovering AL, Bui NK, Uchida K, Aizawa S-I, Vollmer W, Sockett RE. 2012.
522 Specialized peptidoglycan hydrolases sculpt the intra-bacterial niche of predatory
523 *Bdellovibrio* and increase population fitness. PLOS Pathogens 8:e1002524.

524 15. Dashiff A, Junka RA, Libera M, Kadouri DE. 2011. Predation of human pathogens by the
525 predatory bacteria *Micavibrio aeruginosavorus* and *Bdellovibrio bacteriovorus*. Journal of
526 Applied Microbiology 110:431–444.

527 16. Jurkevitch E, Minz D, Ramati B, Barel G. 2000. Prey range characterization, ribotyping,
528 and diversity of soil and rhizosphere *Bdellovibrio* spp. isolated on phytopathogenic bacteria.
529 Appl Environ Microbiol 66:2365–2371.

530 17. Chanyi RM, Ward C, Pechey A, Koval SF. 2013. To invade or not to invade: two
531 approaches to a prokaryotic predatory life cycle. Can J Microbiol 59:273–279.

532 18. Rogosky AM, Moak PL, Emmert EAB. 2006. Differential predation by *Bdellovibrio*
533 *bacteriovorus* 109J. Curr Microbiol 52:81–85.

534 19. Rendulic S, Jagtap P, Rosinus A, Eppinger M, Baar C, Lanz C, Keller H, Lambert C, Evans
535 KJ, Goesmann A, Meyer F, Sockett RE, Schuster SC. 2004. A predator unmasked: life
536 cycle of *Bdellovibrio bacteriovorus* from a genomic perspective. Science 303:689–692.

537 20. Negus D, Moore C, Baker M, Raghunathan D, Tyson J, Sockett RE. 2017. Predator versus
538 pathogen: How does predatory *Bdellovibrio bacteriovorus* interface with the challenges of
539 killing Gram-negative pathogens in a host setting? Annu Rev Microbiol 71:441–457.

540 21. Hoeniger JFM, Ladwig R, Moor H. 1972. The fine structure of "resting bodies" of
541 *Bdellovibrio* sp. strain W developed in *Rhodospirillum rubrum*. Can J Microbiol 18:87–92.

542 22. Oyedara OO, Segura-Cabrera A, Guo X, Elufisan TO, Cantú González RA, Rodríguez
543 Pérez MA. 2018. Whole-genome sequencing and comparative genome analysis provided
544 insight into the predatory features and genetic diversity of two *Bdellovibrio* species isolated
545 from soil. Int J Genomics 2018.

546 23. Enos BG, Anthony MK, DeGiorgis JA, Williams LE. 2018. Prey range and genome
547 evolution of *Halobacteriovorax marinus* predatory bacteria from an estuary. mSphere
548 3:e00508-17.

549 24. Marchesi JR, Sato T, Weightman AJ, Martin TA, Fry JC, Hiom SJ, Dymock D, Wade WG.
550 1998. Design and evaluation of useful bacterium-specific PCR primers that amplify genes
551 coding for bacterial 16S rRNA. Appl Environ Microbiol 64:795–799.

552 25. Heuer H, Krsek M, Baker P, Smalla K, Wellington EM. 1997. Analysis of actinomycete
553 communities by specific amplification of genes encoding 16S rRNA and gel-electrophoretic
554 separation in denaturing gradients. Appl Environ Microbiol 63:3233–3241.

555 26. Ewing B, Green P. 1998. Base-calling of automated sequencer traces using Phred. II. Error
556 probabilities. Genome Res 8:186–194.

557 27. Ewing B, Hillier L, Wendl MC, Green P. 1998. Base-calling of automated sequencer traces
558 using Phred. I. Accuracy assessment. Genome Res 8:175–185.

559 28. Gordon D, Abajian C, Green P. 1998. Consed: A graphical tool for sequence finishing.
560 Genome Res 8:195–202.

561 29. Altschul SF, Gish W, Miller W, Myers EW, Lipman DJ. 1990. Basic local alignment search
562 tool. Journal of Molecular Biology 215:403–410.

563 30. Pruesse E, Peplies J, Glöckner FO. 2012. SINA: Accurate high-throughput multiple
564 sequence alignment of ribosomal RNA genes. Bioinformatics 28:1823–1829.

565 31. Wang Q, Garrity GM, Tiedje JM, Cole JR. 2007. Naïve Bayesian classifier for rapid
566 assignment of rRNA sequences into the new bacterial taxonomy. Appl Environ Microbiol
567 73:5261–5267.

568 32. Jurkevitch E. 2012. Isolation and classification of *Bdellovibrio* and Like Organisms.
569 Current Protocols in Microbiology 7B.1.1-7B.1.20.

570 33. Koval SF. 2007. The search for hunters: culture-dependent and -independent methods for
571 analysis of *Bdellovibrio* and Like Organisms, p. 191–211. *In* Jurkevitch, E (ed.), Predatory
572 Prokaryotes: Biology, Ecology and Evolution. Springer Berlin Heidelberg, Berlin,
573 Heidelberg.

574 34. Cerra J, Donohue H, Kral A, Oser M, Rostkowski L, Zappia L, Williams LE. 2018.
575 Complete genome sequence of *Pseudomonas* sp. strain NC02, isolated from soil. Genome
576 Announc 6.

577 35. Kozlov A, Darriba D, Flouri T, Morel B, Stamatakis A. 2018. RAxML-NG: A fast, scalable,
578 and user-friendly tool for maximum likelihood phylogenetic inference. bioRxiv 447110.

579 36. Rodriguez-R LM, Konstantinidis KT. 2016. The enveomics collection: a toolbox for
580 specialized analyses of microbial genomes and metagenomes. PeerJ Preprints 4:e1900v1.

581 37. Casale A, Clark S, Grasso M, Kryschuk M, Ritzer L, Trudeau M, Williams LE. 2018.
582 Complete genome sequence of *Escherichia coli* ML35. Genome Announc 6.

583 38. Chin C-S, Alexander DH, Marks P, Klammer AA, Drake J, Heiner C, Clum A, Copeland A,
584 Huddleston J, Eichler EE, Turner SW, Korlach J. 2013. Nonhybrid, finished microbial
585 genome assemblies from long-read SMRT sequencing data. Nature Methods 10:563–569.

586 39. Li H, Durbin R. 2009. Fast and accurate short read alignment with Burrows–Wheeler
587 transform. Bioinformatics 25:1754–1760.

588 40. Li H, Handsaker B, Wysoker A, Fennell T, Ruan J, Homer N, Marth G, Abecasis G, Durbin
589 R. 2009. The Sequence Alignment/Map format and SAMtools. Bioinformatics 25:2078–
590 2079.

591 41. Walker BJ, Abeel T, Shea T, Priest M, Abouelliel A, Sakthikumar S, Cuomo CA, Zeng Q,
592 Wortman J, Young SK, Earl AM. 2014. Pilon: An integrated tool for comprehensive
593 microbial variant detection and genome assembly improvement. PLOS ONE 9:e112963.

594 42. Milne I, Stephen G, Bayer M, Cock PJA, Pritchard L, Cardle L, Shaw PD, Marshall D.
595 2013. Using Tablet for visual exploration of second-generation sequencing data. Brief
596 Bioinform 14:193–202.

597 43. Aziz RK, Bartels D, Best AA, DeJongh M, Disz T, Edwards RA, Formsma K, Gerdes S,
598 Glass EM, Kubal M, Meyer F, Olsen GJ, Olson R, Osterman AL, Overbeek RA, McNeil
599 LK, Paarmann D, Paczian T, Parrello B, Pusch GD, Reich C, Stevens R, Vassieva O,
600 Vonstein V, Wilke A, Zagnitko O. 2008. The RAST Server: rapid annotations using
601 subsystems technology. BMC Genomics 9:75.

602 44. Overbeek R, Olson R, Pusch GD, Olsen GJ, Davis JJ, Disz T, Edwards RA, Gerdes S,
603 Parrello B, Shukla M, Vonstein V, Wattam AR, Xia F, Stevens R. 2014. The SEED and the

604 Rapid Annotation of microbial genomes using Subsystems Technology (RAST). Nucleic
605 Acids Res 42:D206-214.

606 45. Nawrocki EP, Eddy SR. 2013. Infernal 1.1: 100-fold faster RNA homology searches.
607 Bioinformatics 29:2933–2935.

608 46. Lowe TM, Chan PP. 2016. tRNAscan-SE On-line: integrating search and context for
609 analysis of transfer RNA genes. Nucleic Acids Res 44:W54-57.

610 47. Lowe TM, Eddy SR. 1997. tRNAscan-SE: a program for improved detection of transfer
611 RNA genes in genomic sequence. Nucleic Acids Res 25:955–964.

612 48. Alikhan N-F, Petty NK, Ben Zakour NL, Beatson SA. 2011. BLAST Ring Image Generator
613 (BRIG): simple prokaryote genome comparisons. BMC Genomics 12:402.

614 49. Lambert C, Sockett RE. 2008. Laboratory maintenance of *Bdellovibrio*. Current Protocols
615 in Microbiology 9:7B.2.1-7B.2.13.

616 50. Stackebrandt E, Goebel BM. 1994. Taxonomic note: A place for DNA-DNA reassociation
617 and 16S rRNA sequence analysis in the present species definition in bacteriology.
618 International Journal of Systematic and Evolutionary Microbiology 44:846–849.

619 51. Stackebrandt E, Ebers J. 2006. Taxonomic parameters revisited: tarnished gold standards.
620 Microbiology Today 33:152–155.

621 52. Ravenhall M, Škunca N, Lassalle F, Dessimoz C. 2015. Inferring horizontal gene transfer.
622 PLoS Comput Biol 11.

623 53. Gophna U, Charlebois RL, Doolittle WF. 2006. Ancient lateral gene transfer in the
624 evolution of *Bdellovibrio bacteriovorus*. Trends Microbiol 14:64–69.

625 54. Pan A, Chanda I, Chakrabarti J. 2011. Analysis of the genome and proteome composition
626 of *Bdellovibrio bacteriovorus*: indication for recent prey-derived horizontal gene transfer.
627 Genomics 98:213–222.

628 55. Hobley L, Lerner TR, Williams LE, Lambert C, Till R, Milner DS, Basford SM, Capeness
629 MJ, Fenton AK, Atterbury RJ, Harris MATS, Sockett RE. 2012. Genome analysis of a
630 simultaneously predatory and prey-independent, novel *Bdellovibrio bacteriovorus* from the
631 River Tiber, supports in silico predictions of both ancient and recent lateral gene transfer
632 from diverse bacteria. BMC Genomics 13:670.

633 56. Fratamico PM, Whiting RC. 1995. Ability of *Bdellovibrio bacteriovorus* 109J to lyse
634 Gram-negative food-borne pathogenic and spoilage bacteria. Journal of Food Protection
635 58:160–164.

636 57. Baker M, Negus D, Raghunathan D, Radford P, Moore C, Clark G, Diggle M, Tyson J,
637 Twycross J, Sockett RE. 2017. Measuring and modelling the response of *Klebsiella*
638 *pneumoniae* KPC prey to *Bdellovibrio bacteriovorus* predation, in human serum and
639 defined buffer. Sci Rep 7:8329.

640 58. Shemesh Y, Jurkevitch E. 2004. Plastic phenotypic resistance to predation by *Bdellovibrio*
641 and like organisms in bacterial prey. Environ Microbiol 6:12–18.

642 59. Cotter TW, Thomashow MF. 1992. Identification of a *Bdellovibrio bacteriovorus* genetic
643 locus, *hit*, associated with the host-independent phenotype. J Bacteriol 174:6018–6024.

644 60. Roschanski N, Klages S, Reinhardt R, Linscheid M, Strauch E. 2011. Identification of
645 genes essential for prey-independent growth of *Bdellovibrio bacteriovorus* HD100. Journal
646 of Bacteriology 193:1745–1756.

647 **Figures and Figure Legends**

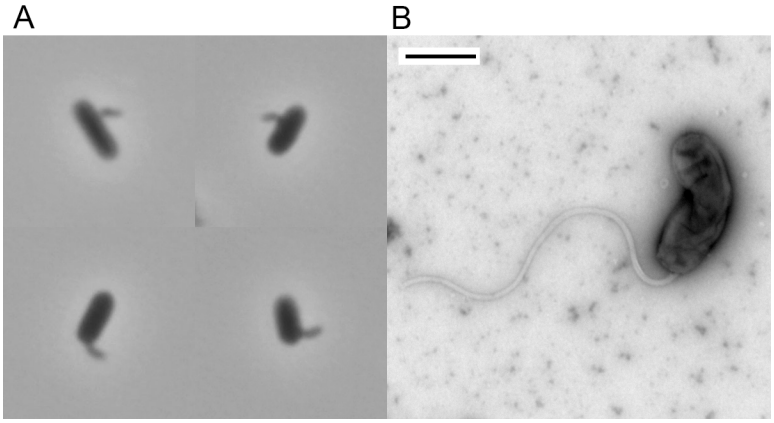

648

649 **Figure 1.** Microscopy of *Bdellovibrio* sp. NC01 isolated from bioswale soil. (A) Compilation of
650 four images taken using 1000x phase-contrast microscopy to show small, comma-shaped NC01
651 attack phase cells attached to larger *E. coli* ML35 cells after 48 hours of co-culture. (B) Negative
652 stain electron microscopy of a NC01 attack phase cell. The scale bar is 500 nm.

653

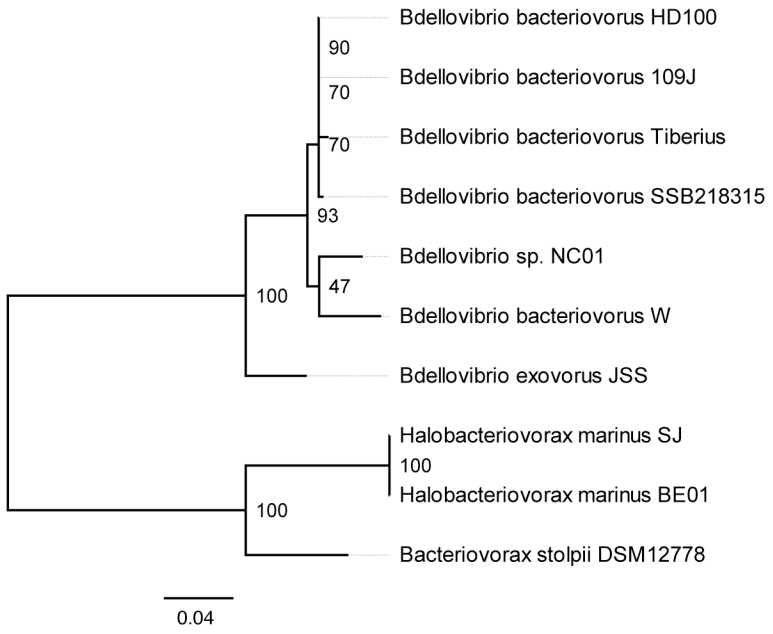

Figure 2. 16S rRNA gene phylogeny. We aligned 16S rRNA gene sequences using SINA 1.2.11, then constructed a phylogeny using RAxML BlackBox with 100 bootstrap replicates. The phylogeny is rooted on the branch joining *Bdellovibrio* with *Bacteriovorax*/*Halobacteriovorax*, and bootstrap support for each node is shown.

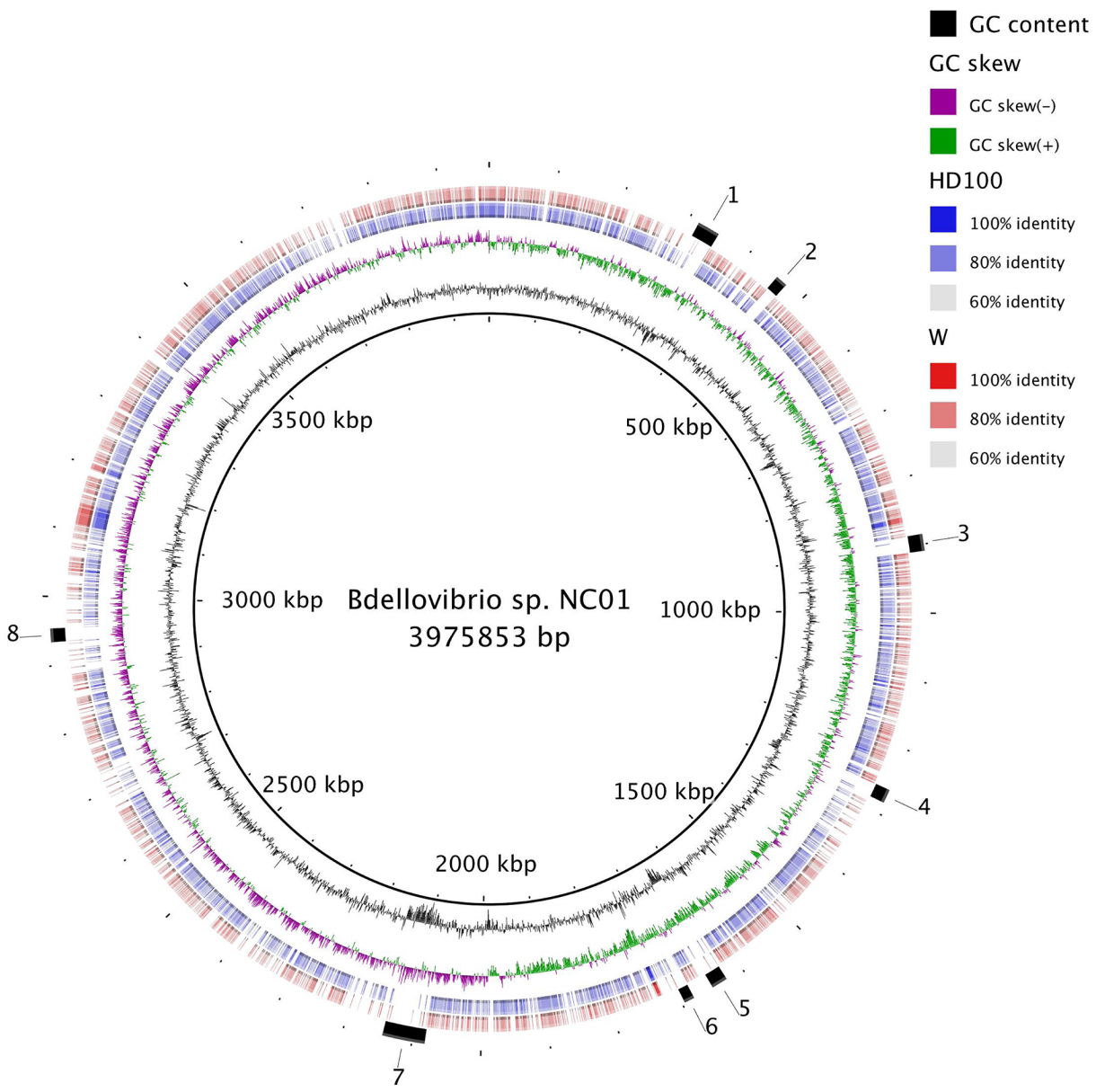

Figure 3. Genome-wide pairwise comparisons of *Bdellovibrio* nucleotide sequences. The genome of *Bdellovibrio* sp. NC01 is shown as the innermost ring. The next ring is a plot of GC content and the purple and green ring is a plot of GC skew, both of which were generated by the BLAST Ring Image Generator (BRIG) using sliding windows to determine deviation from the average value for the genome. The blue ring and red ring show pairwise nucleotide sequence alignments of NC01 to HD100 and W, respectively. Each individual alignment is shown as a block along the ring, and color gradation of the blocks reflects the percent similarity of

667 alignments. The outermost ring denotes eight regions lacking alignments, which may indicate

668 unique NC01 gene content.

669

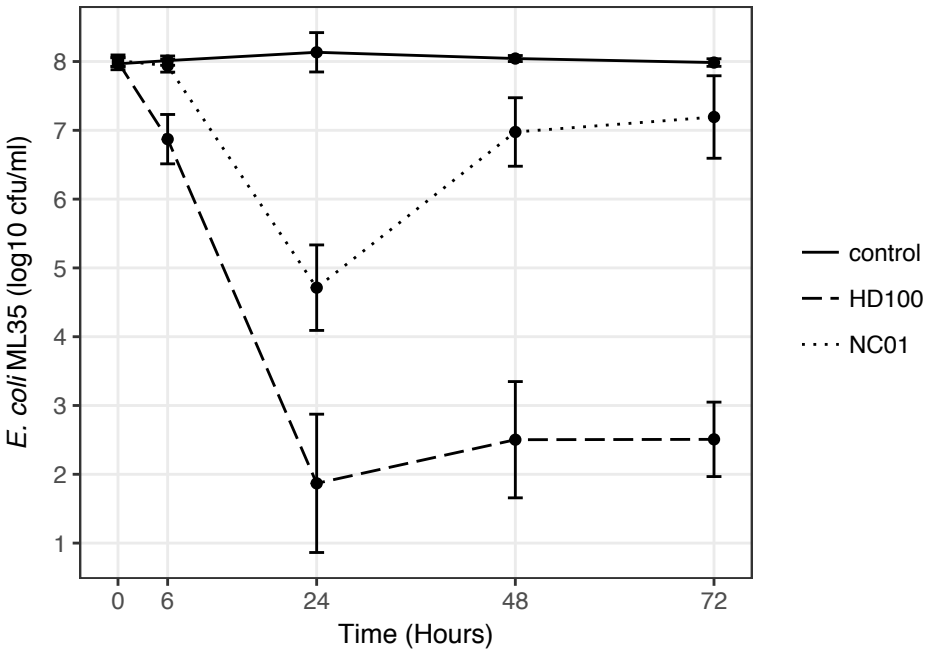

670

671 **Figure 4.** Efficiency of *Bdellovibrio* sp. NC01 and *B. bacteriovorus* HD100 predation on *E. coli*

672 ML35. We quantified viable *E. coli* ML35 over 72 hours on its own (control), combined with

673 *Bdellovibrio* sp. NC01 (NC01) and combined with *B. bacteriovorus* HD100 (HD100). The

674 resulting cfu/ml data were log transformed and plotted using ggplot in RStudio. Each time point

675 shows the mean and standard deviation for at least five replicates.

676

677 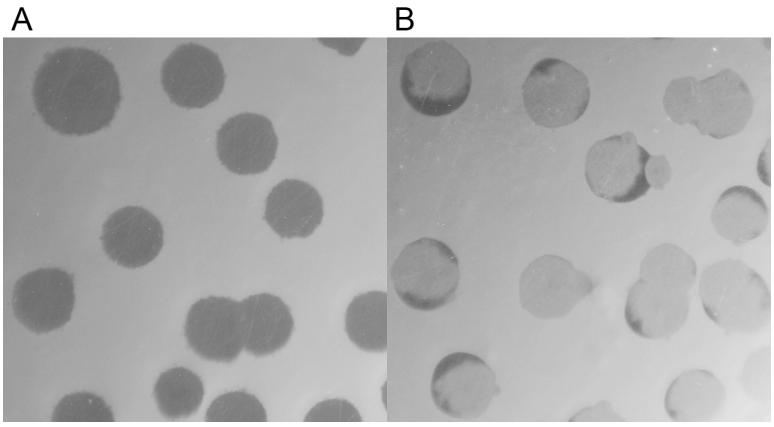

678 **Figure 5.** Plaque phenotypes of *Bdellovibrio* sp. NC01 and *B. bacteriovorus* HD100. Using a
679 double agar overlay method, we assessed plaque formation on lawns of *E. coli* ML35. These
680 images were taken after 6 days of incubation and illustrate reproducible differences in the
681 appearance of plaques formed by HD100 (A) and NC01 (B).
682

683 **Tables**

684 Table 1. Average amino acid identity among *Bdellovibrio* genomes

	NC01	W	HD100	109J
NC01		64.4	68.8	68.8
W	64.4		66.4	66.5
HD100	68.8	66.4		99.2
109J	68.8	66.5	99.2	

685

686 Table 2. Genome comparison of *Bdellovibrio* sp. NC01, *Bdellovibrio bacteriovorus* HD100 and
687 *Bdellovibrio bacteriovorus* W
688

	Bdellovibrio sp. NC01		*Bdellovibrio bacteriovorus* HD100		*Bdellovibrio bacteriovorus* W	
	PGAP	RAST and RFAM/ tRNAScan	PGAP	RAST and RFAM/ tRNAScan	PGAP	RAST and RFAM/ tRNAScan
Genome size (bp)	3,975,853		3,782,950		3,006,992	
GC content (%)	44.5		50.6		43.3	
Genes	3,840	3,828	3,597	3,651	2,834	2,901
Protein-coding	3,773	3,776	3,548	3,597	2,760	2,849
Hypothetical proteins	1,712	1,431	1,245	1,309	962	971
tRNA	34	34	36	36	34	34
rRNA	6	6	6	6	6	6
Other RNA	4	12	4	12	4	12

689

690 Table 3. Prey range of *B. bacteriovorus* HD100 and *Bdellovibrio* sp. NC01

Genus	Strain ID	Environment	Plaque formation[a]	
			HD100	NC01
Acinetobacter	0036	Freshwater	Yes	No
Aeromonas	0031	Freshwater	Yes	Yes
Enterobacteriaceae	0032	Freshwater	Yes	Yes
Raoultella	0037	Freshwater	Yes	No
Pseudomonas	NC02 (0042)[b]	Soil	Yes	Yes
Serratia	0043	Soil	Yes	Yes
Escherichia	0057		Yes	No
Escherichia	ML35		Yes	Yes

691 [a]Plaque formation data based on three replicates

692 [b]*Pseudomonas* sp. NC02 is referred to as 0042 in (23)

693